

## Puzzle with the precession of the neutron spin

V. Sulkosky,<sup>1,2,3</sup> C. Peng,<sup>4,5</sup> J.-P. Chen,<sup>2</sup> A. Deur\*,<sup>3,2</sup> S. Abrahamyan,<sup>6</sup> K. A. Aniol,<sup>7</sup>  
D. S. Armstrong,<sup>1</sup> T. Averett,<sup>1</sup> S. L. Bailey,<sup>1</sup> A. Beck,<sup>8</sup> P. Bertin,<sup>9</sup> F. Butaru,<sup>10</sup>  
W. Boeglin,<sup>11</sup> A. Camsonne,<sup>9</sup> G. D. Cates,<sup>3</sup> C. C. Chang,<sup>12</sup> Seonho Choi,<sup>10</sup> E. Chudakov,<sup>2</sup>  
L. Coman,<sup>11</sup> J. C. Cornejo,<sup>7</sup> B. Craver,<sup>3</sup> F. Cusanno,<sup>13</sup> R. De Leo,<sup>14</sup> C. W. de Jager<sup>†</sup>,<sup>2</sup>  
J. D. Denton,<sup>15</sup> S. Dhamija,<sup>16</sup> R. Feuerbach,<sup>2</sup> J. M. Finn<sup>†</sup>,<sup>1</sup> S. Frullani<sup>†</sup>,<sup>17,18</sup> K. Fuoti,<sup>1</sup>  
H. Gao,<sup>4</sup> F. Garibaldi,<sup>17,18</sup> O. Gayou,<sup>8</sup> R. Gilman,<sup>2,19</sup> A. Glamazdin,<sup>20</sup> C. Glashauser,<sup>19</sup>  
J. Gomez,<sup>2</sup> J.-O. Hansen,<sup>2</sup> D. Hayes,<sup>21</sup> B. Hersman,<sup>22</sup> D. W. Higinbotham,<sup>2</sup>  
T. Holmstrom,<sup>1,15</sup> T. B. Humensky,<sup>3</sup> C. E. Hyde,<sup>21</sup> H. Ibrahim,<sup>21,23</sup> M. Iodice,<sup>13</sup> X. Jiang,<sup>19</sup>  
L. J. Kaufman,<sup>24</sup> A. Kelleher,<sup>1</sup> K. E. Keister,<sup>1</sup> W. Kim,<sup>25</sup> A. Kolarkar,<sup>16</sup> N. Kolb,<sup>26</sup>  
W. Korsch,<sup>16</sup> K. Kramer,<sup>1,4</sup> G. Kumbartzki,<sup>19</sup> L. Lagamba,<sup>14</sup> V. Lainé,<sup>2,9</sup> G. Laveissiere,<sup>9</sup>  
J. J. Lerose,<sup>2</sup> D. Lhuillier,<sup>27</sup> R. Lindgren,<sup>3</sup> N. Liyanage,<sup>3,2</sup> H.-J. Lu,<sup>28</sup> B. Ma,<sup>8</sup>  
D. J. Margaziotis,<sup>7</sup> P. Markowitz,<sup>11</sup> K. McCormick,<sup>19</sup> M. Meziane,<sup>4</sup> Z.-E. Meziani,<sup>10</sup>  
R. Michaels,<sup>2</sup> B. Moffit,<sup>1</sup> P. Monaghan,<sup>8</sup> S. Nanda,<sup>2</sup> J. Niedziela,<sup>24</sup> M. Niskin,<sup>11</sup>  
R. Pandolfi,<sup>29</sup> K. D. Paschke,<sup>24</sup> M. Potokar<sup>†</sup>,<sup>30</sup> A. Puckett,<sup>3</sup> V. A. Punjabi,<sup>31</sup> Y. Qiang,<sup>8</sup>  
R. Ransome,<sup>19</sup> B. Reitz,<sup>2</sup> R. Roché,<sup>32</sup> A. Saha<sup>†</sup>,<sup>2</sup> A. Shabetai,<sup>19</sup> S. Širca,<sup>33</sup> J. T. Singh,<sup>3</sup>  
K. Slifer,<sup>10</sup> R. Snyder,<sup>3</sup> P. Solvignon<sup>†</sup>,<sup>10</sup> R. Stringer,<sup>4</sup> R. Subedi,<sup>34</sup> W. A. Tobias,<sup>3</sup> N. Ton,<sup>3</sup>  
P. E. Ulmer,<sup>21</sup> G. M. Urciuoli,<sup>13</sup> A. Vacheret,<sup>27</sup> E. Voutier,<sup>35</sup> K. Wang,<sup>3</sup> L. Wan,<sup>8</sup>  
B. Wojtsekhowski,<sup>36</sup> S. Woo,<sup>25</sup> H. Yao,<sup>10</sup> J. Yuan,<sup>19</sup> X. Zhan,<sup>8</sup> X. Zheng,<sup>5</sup> and L. Zhu<sup>8</sup>

(Jefferson Lab E97-110 Collaboration)

<sup>1</sup>*College of William and Mary, Williamsburg, Virginia 23187-8795, USA*

<sup>2</sup>*Thomas Jefferson National Accelerator Facility, Newport News, Virginia 23606, USA*

<sup>3</sup>*University of Virginia, Charlottesville, Virginia 22904, USA*

<sup>4</sup>*Duke University, Durham, North Carolina 27708, USA*

---

\* Corresponding author; E-mail: [deurpam@jlab.org](mailto:deurpam@jlab.org).

<sup>†</sup> Deceased.

- <sup>5</sup>*Argonne National Laboratory, Argonne, Illinois 60439, USA*
- <sup>6</sup>*Yerevan Physics Institute, Yerevan 375036, Armenia*
- <sup>7</sup>*California State University, Los Angeles, Los Angeles, California 90032, USA*
- <sup>8</sup>*Massachusetts Institute of Technology, Cambridge, Massachusetts 02139, USA*
- <sup>9</sup>*LPC Clermont-Ferrand, Université Blaise Pascal, CNRS/IN2P3, F-63177 Aubière, France*
- <sup>10</sup>*Temple University, Philadelphia, Pennsylvania 19122, USA*
- <sup>11</sup>*Florida International University, Miami, Florida 33199, USA*
- <sup>12</sup>*University of Maryland, College Park, Maryland 20742, USA*
- <sup>13</sup>*Istituto Nazionale di Fisica Nucleare, Sezione di Roma,  
Piazzale A. Moro 2, I-00185 Rome, Italy*
- <sup>14</sup>*Istituto Nazionale di Fisica Nucleare, Sezione di Bari and University of Bari, I-70126 Bari, Italy*
- <sup>15</sup>*Longwood University, Farmville, VA 23909, USA*
- <sup>16</sup>*University of Kentucky, Lexington, Kentucky 40506, USA*
- <sup>17</sup>*Istituto Nazionale di Fisica Nucleare, Sezione di Roma, I-00185 Rome, Italy*
- <sup>18</sup>*Istituto Superiore di Sanità, I-00161 Rome, Italy*
- <sup>19</sup>*Rutgers, The State University of New Jersey, Piscataway, New Jersey 08855, USA*
- <sup>20</sup>*Kharkov Institute of Physics and Technology, Kharkov 310108, Ukraine*
- <sup>21</sup>*Old Dominion University, Norfolk, Virginia 23529, USA*
- <sup>22</sup>*University of New Hampshire, Durham, New Hampshire 03824, USA*
- <sup>23</sup>*Cairo University, Cairo, Giza 12613, Egypt*
- <sup>24</sup>*University of Massachusetts-Amherst, Amherst, Massachusetts 01003, USA*
- <sup>25</sup>*Kyungpook National University, Taegu City, South Korea*
- <sup>26</sup>*University of Saskatchewan, Saskatoon, SK S7N 5E2, Canada*
- <sup>27</sup>*DAPNIA/SPhN, CEA Saclay, F-91191 Gif-sur-Yvette, France*
- <sup>28</sup>*Department of Modern Physics, University of Science and Technology of China, Hefei 230026, China*
- <sup>29</sup>*Randolph-Macon College, Ashland, Virginia 23005, USA*
- <sup>30</sup>*Institut Jozef Stefan, University of Ljubljana, Ljubljana, Slovenia*
- <sup>31</sup>*Norfolk State University, Norfolk, Virginia 23504, USA*

<sup>32</sup>*Florida State University, Tallahassee, Florida 32306, USA*

<sup>33</sup>*Faculty of Mathematics and Physics, University of Ljubljana, Slovenia*

<sup>34</sup>*Kent State University, Kent, Ohio 44242, USA*

<sup>35</sup>*LPSC, Université Joseph Fourier, CNRS/IN2P3, INPG, F-38026 Grenoble, France*

<sup>36</sup>*Thomas Jefferson National Accelerator Facility, Newport News, Virginia 23606, USA*

(Dated: October 22, 2020)

Understanding the structure of the nucleon (proton and neutron) is a critical problem in physics. Especially challenging is to understand the spin structure when the Strong Interaction becomes truly strong. At energy scales below the nucleon mass ( $\sim 1$  GeV), the intense interactions of the quarks and gluons inside the nucleon makes them highly correlated. Their coherent behavior causes the emergence of effective hadronic degrees of freedom (hadrons are composite particles made of quarks and gluons) which are necessary to understand the nucleon properties. Theoretically studying this subject requires approaches employing non-perturbative techniques or using hadronic degrees of freedom, e.g. chiral effective field theory ( $\chi$ EFT) [1]. Here, we present measurements sensitive to the neutron's spin precession under electromagnetic fields. The observables, the generalized spin-polarizabilities  $\delta_{LT}$  and  $\gamma_0$ , which quantify the nucleon spin's precession, were measured at very low energy-momentum transfer squared  $Q^2$  corresponding to probing distances of the size of the nucleon. Our  $Q^2$  values match the domain where  $\chi$ EFT calculations are expected to be applicable. The calculations have been conducted to high degrees of sophistication [2–4], including that of the so-called “gold-plated” observable–  $\delta_{LT}$ . Surprisingly however, our data show a strong discrepancy with the  $\chi$ EFT calculations. This presents a challenge to the current description of the neutron's spin properties.

The nucleon is the basic building block of nature, accounting for about 99% of the uni-

verse's visible mass. Understanding its properties, e.g., mass and spin, is thus crucial. Those are mainly determined by the Strong Interaction, which is described by Quantum Chromodynamics (QCD) with quarks and gluons as the fundamental degrees of freedom. The nucleon structure is satisfactorily understood at high  $Q^2$  (short space-time scales) since there, QCD is calculable using perturbation methods (perturbative QCD) and tested by numerous experimental measurements. At lower  $Q^2$ , the strong coupling  $\alpha_s$  becomes too large for perturbative QCD to be applicable [5]. Yet, calculations are critically needed since there the Strong Interaction's chiral symmetry breaks, which is believed to lead to the emergence of the nucleon's global properties. To understand these properties, non-perturbative methods must be used. A method using the fundamental quark and gluon degrees of freedom is lattice QCD. However, calculations from this method are often intractable for spin observables at low  $Q^2$  [6]. Another solution is to employ effective theories.  $\chi$ EFT capitalizes on QCD's approximate chiral symmetry and uses the emergent hadronic degrees of freedom. Therein lies  $\chi$ EFT's strengths and challenges: while the nucleon and the pion are used for first-order calculations, this is often insufficient to describe the data, and heavier hadrons, such as the nucleon's first excited state  $\Delta(1232)$ , become needed. This complicates  $\chi$ EFT calculations, and theorists are still seeking the best way to include the  $\Delta(1232)$  in their calculations. It is therefore crucial to perform precision measurements at low enough  $Q^2$  to test  $\chi$ EFT calculations. Spin observables, among them the generalized spin-polarizabilities that are reported here, provide an extensive set of tests to benchmark  $\chi$ EFT calculations [6].

Polarizabilities describe how the components of an object collectively react to external electromagnetic fields. In particular, spin-polarizabilities quantify the object's spin precession under an electromagnetic field, see Fig. 1. The spin-polarizabilities, initially defined with real photons, can be generalized to virtual photons such as those used to probe the neutron in our experiment (see Fig. 2). The energy-momentum transferred between the electron and neu-

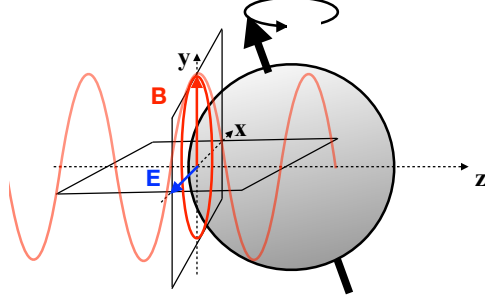


FIG. 1: *Spin-polarizabilities* quantify the precession (curled black arrow) of the spin of the neutron (black arrow and gray sphere, respectively) under electromagnetic fields (electric field  $\mathbf{E}$ : blue arrow; magnetic field  $\mathbf{B}$ : red arrow). Electromagnetic waves formed by real photons have  $\mathbf{E}$  and  $\mathbf{B}$  and polarization vectors perpendicular to the wave propagation direction  $\mathbf{z}$ . *Generalized* spin-polarizabilities arise with virtual photons which also have a longitudinal polarization component.

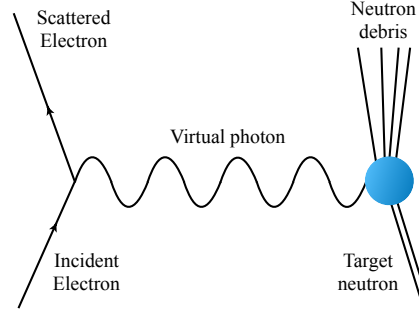


FIG. 2: Electron scattering off a neutron by the one-photon exchange process. If both the incident electron and the neutron are polarized, this process can be used to measure the generalized spin-polarizabilities of the neutron.

tron is  $(\nu, \mathbf{q})$ , with  $Q^2 = \mathbf{q}^2 - \nu^2$  characterizing the space-time scale at which we probe the neutron. While real photons ( $Q^2 = 0$ ) only have transverse polarizations, mediating virtual photons ( $Q^2 \neq 0$ ) are transversely (T) or longitudinally (L) polarized. Thus, two contributions to the spin-polarizability arise, one from the transverse-transverse (TT) interference called the forward spin-polarizability  $\gamma_0(Q^2)$ , and the other from the longitudinal-transverse (LT) interfer-

ence, called the Longitudinal-Transverse interference polarizability  $\delta_{\text{LT}}(Q^2)$  and available only with virtual photons. The additional polarization direction L and the ensuing interference term offer extra latitude to test theories describing the Strong Interaction.

The theoretical basis to measure  $\delta_{\text{LT}}(Q^2)$  originates from a work of Gell-Mann, Goldberger and Thirring [7, 8]. This work lead relations between the cross-sections measured in polarized electron-nucleon scattering (Fig. 2) and the spin-polarizabilities:

$$\gamma_0(Q^2) = \frac{1}{2\pi^2} \int_{\nu_0}^{\infty} \frac{\kappa_\gamma}{\nu^2} \frac{\sigma_{\text{TT}}(\nu, Q^2)}{\nu^2} d\nu, \quad (1)$$

$$\delta_{\text{LT}}(Q^2) = \left( \frac{1}{2\pi^2} \right) \int_{\nu_0}^{\infty} \frac{\kappa_\gamma}{\nu Q} \frac{\sigma_{\text{LT}}(\nu, Q^2)}{\nu^2} d\nu, \quad (2)$$

where  $\sigma_{\text{TT}}$  and  $\sigma_{\text{LT}}$  are respectively the TT and LT interference cross-section,  $\kappa_\gamma = \nu - Q^2/2M$  [9] is the photon flux factor with  $\nu$  the energy transfer and  $\nu_0$  the photoproduction threshold. The  $\nu^{-2}$  weighting factor facilitates the convergence of the integral and minimizes the issue that  $\nu \rightarrow \infty$  cannot be reached experimentally.

An outstanding feature of  $\delta_{\text{LT}}(Q^2)$  at low  $Q^2$  is that the  $\Delta(1232)$  is not expected to significantly contribute to the LT-interference cross section, since exciting the  $\Delta(1232)$  overwhelmingly involves transverse photons. This should alleviate the difficulty of including the  $\Delta(1232)$  in  $\chi\text{EFT}$  calculations, making them more robust. However, the first measurement of  $\delta_{\text{LT}}(Q^2)$  from JLab experiment E94-010 [12] done at  $Q^2 \geq 0.1 \text{ GeV}^2$  strongly disagreed with  $\chi\text{EFT}$  calculations [10, 11]. This surprising result, known as the “ $\delta_{\text{LT}}$  puzzle” [13], triggered improved  $\chi\text{EFT}$  calculations [14] which now explicitly include the  $\Delta(1232)$  [2–4], and measurements of  $\delta_{\text{LT}}$  at lower  $Q^2$  where  $\chi\text{EFT}$  can be best tested. New data of  $\delta_{\text{LT}}$  on the neutron at very low  $Q^2$ , taken during experiment JLab E97-110, are presented next.

Eq. (2) allows measuring  $\delta_{\text{LT}}^n(Q^2)$  (the superscript  $n$  indicates neutron quantities) by scattering polarized electrons off polarized neutrons in  $^3\text{He}$  nuclei. The measured cross-section

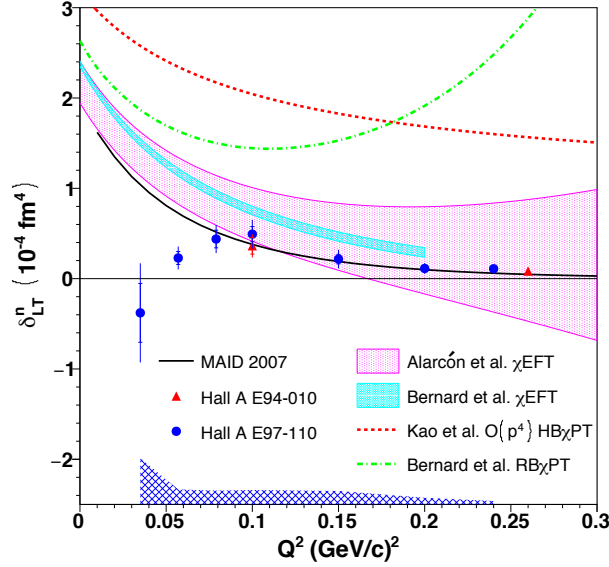


FIG. 3:  $\delta_{LT}^n(Q^2)$  from experiment E97-110, compared to earlier E94-010 data [12],  $\chi$ EFT calculations [2, 4, 10, 11] and the MAID model [15]. The inner error bars, sometimes too small to be visible, represent the statistical uncertainties. The outer error bars show the combined statistical and uncorrelated systematic uncertainties. The correlated systematic uncertainty is indicated by the band at the bottom.

$\sigma_{LT}(\nu, Q^2)$  is used with Eq. (2) to form  $\delta_{LT}^n(Q^2)$ , after which nuclear corrections are applied (see supplemental material). Our data are shown in Fig. 3. They agree with earlier data from E94-010 at larger  $Q^2$  [12] while reaching much lower  $Q^2$  where the  $\chi$ EFT is expected to work well. The measurement can be compared to  $\chi$ EFT calculations [2, 4, 10, 11] and a model parameterization of the world photo- and electro-production data called MAID [15]. Earlier  $\chi$ EFT calculations [10, 11] used different approaches (Heavy Baryon and Relativistic Baryon chiral perturbation theory: HB $\chi$ PT and RB $\chi$ PT, respectively), and furthermore either neglected the  $\Delta(1232)$  degrees of freedom, or included it approximately. Newer calculations [2–4] account for the  $\Delta(1232)$  explicitly by using a perturbative expansion, but they differ in their choice of expansion parameter. Despite this theoretical improvement and the small  $Q^2$  reach that places our data well in the validity domain of  $\chi$ EFT, our  $\delta_{LT}^n(Q^2)$  starkly disagrees with the predictions.

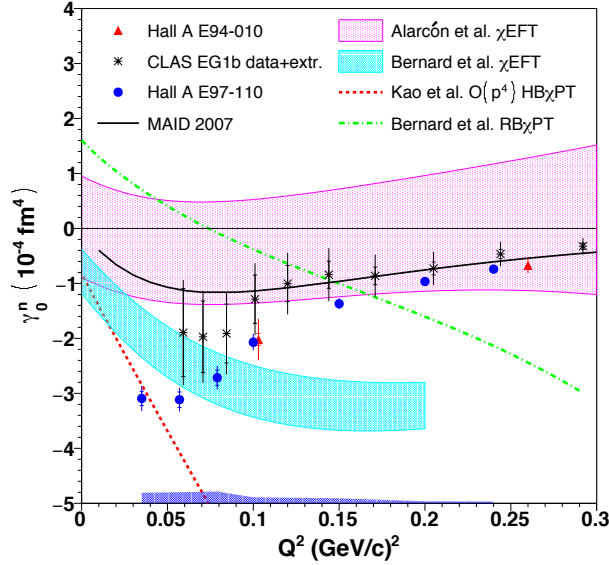


FIG. 4: Same as Fig. 3 but for the other generalized spin-polarizability,  $\gamma_0^n(Q^2)$ .

This is even more surprising because the latest  $\chi$ EFT calculations of  $\delta_{\text{LT}}^n$  agree with each other, suggesting that calculations for this particular observable should be under control. However, our data reveal an opposite trend with  $Q^2$  to that of all the  $\chi$ EFT calculations.

This startling discrepancy demanded further scrutinization of our data. They are compatible with the E94-010 data where they overlap. This is also true for  $\gamma_0^n(Q^2)$ , which we measured concurrently and show in Fig. 4. The measured  $\gamma_0^n(Q^2)$  also agrees with data from CLAS experiment EG1 [16], which used a target and detectors that are very different from E97-110 and E94-010. Our  $\gamma_0^n(Q^2)$  data generally disagree with  $\chi$ EFT calculations. Since  $\gamma_0(Q^2)$  does not benefit from the suppression of the  $\Delta(1232)$  contribution, and since  $\gamma_0^n(Q^2)$  predictions do not reach a consensus, this disagreement is not entirely surprising, in contrast to the unexpected  $\delta_{\text{LT}}^n(Q^2)$  disagreement. Interestingly, we can also study with our data the Schwinger relation [17], which has a similar definition but without  $\nu^{-2}$  weighting in its integrand. The Schwinger integral is shown in Fig. 5 of the Supplemental Materials and displays a similar  $Q^2$ -behavior as  $\delta_{\text{LT}}$ , irrespective of the different  $\nu$ -weighting. Other integrals without  $\nu^{-2}$  weighting



formed using our data and reported in [18] did not display the surprisingly strong disagreements with the predictions seen here.

In conclusion, we measured the spin-polarizability  $\delta_{LT}^n(Q^2)$  well into the domain where  $\chi$ EFT is expected to describe reliably the nucleon properties. Surprisingly, data and predictions disagree significantly. This is perplexing since  $\delta_{LT}$  was expected to be a robust prediction of  $\chi$ EFT and the earlier finding that the  $\Delta(1232)$  is important for the calculation of  $\delta_{LT}$  had been addressed. Our data indicate that both the TT and LT interferences of the electromagnetic field’s components induce a clear spin precession of the neutron. While it was predicted by all calculations and models that the LT term influence should intensify at small  $Q^2$ , our data reveal the opposite trend. Lattice QCD calculations of  $\delta_{LT}(Q^2)$  are possible [19], but not yet available. Our data motivate such calculations since the measured generalized spin-polarizabilities underline a current lack of reliable quantitative descriptions of the Strong Interaction at the nucleon-size scale, even for “gold-plated” observables such as  $\delta_{LT}$ .

**Method Summary** The data were acquired in the Hall A [21] of Jefferson Lab (JLab) during experiment E97-110 [18]. The probing virtual photons were produced by a longitudinally polarized electron beam during its scattering off a polarized  $^3\text{He}$  target [21]. The beam polarization, flipped pseudo-randomly at 30 Hz and monitored by Møller and Compton polarimeters, was  $75.0 \pm 2.3\%$ . The beam energies ranged from 1.1 to 4.4 GeV and the beam current was typically a few  $\mu\text{A}$ . Since free neutrons are unstable we used  $^3\text{He}$  nuclei as an effective polarized neutron target. To first-order, polarized  $^3\text{He}$  nuclei are equivalent to polarized neutrons because the  $^3\text{He}$ ’s nucleons (two protons and one neutron) are mostly in an  $S$ -state, so the Pauli exclusion principle dictates that in the  $S$ -state, the proton spins point oppositely, yielding no net contribution to the  $^3\text{He}$  spin. The gaseous ( $\approx 12$  atm)  $^3\text{He}$  was contained in a 40 cm-long glass cylinder, and polarized by spin-exchange optical pumping of Rubidium atoms. Helmholtz coils provided a parallel or transverse 2.5 mT field used to maintain the polarization, to orient

it longitudinally or perpendicularly (in-plane) to the beam direction, and to aid in performing polarimetry. The average target polarization in-beam was  $(39.0 \pm 1.6)\%$ . The scattered electrons from the reaction  ${}^3\vec{\text{He}}(\vec{e}, e')$  were detected by a High Resolution Spectrometer (HRS) [21] supplemented by a dipole magnet [22] allowing scattering angles down to  $6^\circ$ . Behind the HRS, drift chambers provided particle tracking, scintillator planes enabled the data acquisition trigger, and a gas Cherenkov counter and electromagnetic calorimeters ensured the identification of the particle type. Both spin asymmetries and absolute cross-sections were measured and used to form  $\sigma_{\text{TT}}(\nu, Q^2)$  and  $\sigma_{\text{LT}}(\nu, Q^2)$  [6]. They were integrated according to Eqs. (1) and (2) to obtain the integrals  $\gamma_0^n(Q^2)$  and  $\delta_{\text{LT}}^n(Q^2)$ . The unmeasured part of the integral at large  $\nu$  is negligible for  $\gamma_0^n$  and  $\delta_{\text{LT}}^n$  due to the  $\nu$ -weighting of their integrands. The values  $\gamma_0^n(Q^2)$  and  $\delta_{\text{LT}}^n(Q^2)$  with their uncertainties are provided in the Supplemental Material, as well as the integration range which was covered. While polarized  ${}^3\text{He}$  nuclei are effectively polarized neutrons to good approximation, nuclear corrections are needed to obtain genuine neutron information. The prescription of Ref. [23] was used for the correction. Typically, the correction increases by 20% the absolute values of the generalized spin-polarizabilities except for the lowest  $Q^2$  point for  $\delta_{\text{LT}}^n$  where the correction is smaller, less than 7%. The relative uncertainty on this correction is estimated to be 6 to 14%, the higher uncertainties corresponding to our lowest  $Q^2$  values. The other main systematic uncertainties come from the absolute cross-sections (3.5 to 4.5%), target and beam polarizations (3 to 5% and 3.5%, respectively), and radiative corrections (3 to 7%).

**Data availability** Experimental data that support the findings of this study are provided in the supplemental material or are available from J.P Chen, A. Deur, C. Peng or V. Sulkosky upon request.

**Code availability** The computer codes that support the plots within this paper and the findings of this study are available from J.P Chen, A. Deur, C. Peng or V. Sulkosky upon request.

**Author contributions** The members of the Jefferson Lab E97-110 Collaboration constructed and operated the experimental equipment used in this experiment. All authors contributed to the data collection, experiment design and commissioning, data processing, data analysis or Monte Carlo simulations. The following authors especially contributed to the main data analysis: J.P Chen, C. Peng, A. Deur, and V. Sulkosky.

### Acknowledgments

We acknowledge the outstanding support of the Jefferson Lab Hall A technical staff and the Physics and Accelerator Divisions that made this work possible. We thank A. Deltuva, J. Golak, F. Hagelstein, H. Krebs, V. Lensky, U.-G. Meißner, V. Pascalutsa, G. Salmè, S. Scopetta and M. Vanderhaeghen for useful discussions and for sharing their calculations. We are grateful to V. Pascalutsa and M. Vanderhaeghen for suggesting to compare the data to the Schwinger relation. This material is based upon work supported by the U.S. Department of Energy, Office of Science, Office of Nuclear Physics under contract DE-AC05-06OR23177, and by the NSF under grant PHY-0099557.

- 
- [1] V. Bernard, N. Kaiser and U. G. Meissner, [Int. J. Mod. Phys. E \*\*4\*\*, 193 \(1995\)](#)
  - [2] V. Bernard, E. Epelbaum, H. Krebs and U. G. Meissner, [Phys. Rev. D \*\*87\*\*, no. 5, 054032 \(2013\)](#)
  - [3] V. Lensky, J. M. Alarcón and V. Pascalutsa, [Phys. Rev. C \*\*90\*\*, no. 5, 055202 \(2014\)](#)
  - [4] J. M. Alarcón, F. Hagelstein, V. Lensky and V. Pascalutsa, [arXiv:2006.08626](#)
  - [5] A. Deur, S. J. Brodsky and G. F. de Téramond, [Prog. Part. Nucl. Phys. \*\*90\*\*, 1 \(2016\)](#)
  - [6] A. Deur, S. J. Brodsky and G. F. De Téramond, [Rep. Prog. Phys., \*\*82\*\*, 7 \(2019\)](#)
  - [7] M. Gell-Mann, M. L. Goldberger and W. E. Thirring, [Phys. Rev. \*\*95\*\*, 1612 \(1954\)](#)
  - [8] P. A. M. Guichon, G. Q. Liu and A. W. Thomas, [Nucl. Phys. A \*\*591\*\*, 606 \(1995\)](#)
  - [9] L. N. Hand, [Phys. Rev. \*\*129\*\*, 1834 \(1963\)](#)

- [10] V. Bernard, T. R. Hemmert and U. G. Meissner, [Phys. Rev. D \*\*67\*\*, 076008 \(2003\)](#)
- [11] C. W. Kao, T. Spitzenberg and M. Vanderhaeghen, [Phys. Rev. D \*\*67\*\*, 016001 \(2003\)](#)
- [12] M. Amarian *et al.*, [E94-010 experiment] [Phys. Rev. Lett. \*\*93\*\*, 152301 \(2004\)](#)
- [13] J. P. Chen, [Int. J. Mod. Phys. E \*\*19\*\*, 1893 \(2010\)](#)
- [14] F. Hagelstein, R. Miskimen and V. Pascalutsa, [Prog. Part. Nucl. Phys. \*\*88\*\*, 29-97 \(2016\)](#)
- [15] D. Drechsel, O. Hanstein, S. S. Kamalov and L. Tiator, [Nucl. Phys. A \*\*645\*\*, 145 \(1999\)](#)
- [16] N. Guler *et al.*, [EG1b experiment] [Phys. Rev. C \*\*92\*\*, no. 5, 055201 \(2015\)](#)
- [17] J. S. Schwinger, [Proc. Nat. Acad. Sci. \*\*72\*\*, 1 \(1975\)](#)
- [18] V. Sulkosky *et al.* [E97-110 Collaboration], [Phys. Lett. B \*\*805\*\*, 135428 \(2020\)](#)
- [19] A. J. Chambers *et al.*, [Phys. Rev. Lett. \*\*118\*\*, 24 242001 \(2017\)](#)
- [20] H. Burkhardt and W. N. Cottingham, [Annals Phys. \*\*56\*\*, 453 \(1970\)](#)
- [21] J. Alcorn *et al.*, [Nucl. Instrum. Meth. A \*\*522\*\*, 294 \(2004\)](#)
- [22] F. Garibaldi *et al.* [Phys. Rev. C \*\*99\*\*, 054309 \(2019\)](#)
- [23] C. Ciofi degli Atti and S. Scopetta, [Phys. Lett. B \*\*404\*\*, 223 \(1997\)](#)
- [24] K. P. Adhikari *et al.*, [EG4 experiment] [Phys. Rev. Lett. \*\*120\*\*, 062501 \(2018\)](#)
- [25] S. D. Bass, M. Skurzok and P. Moskal, [Phys. Rev. C \*\*98\*\*, 025209 \(2018\)](#)
- [26] Z. Ye, J. Arrington, R. J. Hill and G. Lee, [Phys. Lett. B \*\*777\*\*, 8-15 \(2018\)](#)
- [27] K. Helbing, [Prog. Part. Nucl. Phys. \*\*57\*\*, 405-469 \(2006\)](#)
- [28] S. B. Gerasimov, [Sov. J. Nucl. Phys. \*\*2\*\*, 430 \(1966\)](#)
- [29] S. D. Drell and A. C. Hearn, [Phys. Rev. Lett. \*\*16\*\*, 908 \(1966\)](#)

## Supplemental material

Verification of the data quality using the Schwinger relation: A relation similar to that of  $\delta_{LT}$  but without  $\nu^{-2}$  weighting is:

$$I_{LT}(Q^2) \equiv \left( \frac{M^2}{\alpha\pi^2} \right) \int_{\nu_0}^{\infty} \left[ \kappa_{\gamma} \frac{\sigma_{LT}(\nu, Q^2)}{Q\nu} \right]_{Q=0} d\nu \quad (3)$$

Schwinger predicted that  $I_{LT}(Q^2) \xrightarrow{Q^2 \rightarrow 0} \kappa e_t$  [17], with  $\kappa$  the summer anomalous magnetic moment of the target particle and  $e_t$  its electric charge. This prediction is general, e.g. it does not use  $\chi$ EFT.  $I_{LT}(Q^2)$  having no  $\nu$ -weighting, the large  $\nu$  contribution to the integral is not negligible. Since this contribution to the integral cannot be measured, a parameterization based on the model described in [24] completed by a Regge-based parameterization [25] for the largest  $\nu$  part was used to extrapolate it. Our measurement of  $I_{LT}^n(Q^2)$  is shown in Fig. 5. Our measurement of  $I_{LT}^n(Q^2)$  without the Regge-based parameterization [25] for the large- $\nu$  part (open symbols), which is suppressed in  $\delta_{LT}(Q^2)$ , displays a similar pattern as  $\delta_{LT}^n(Q^2)$ . The Gerasimov-Drell-Hearn (GDH) relation [28, 29] can be used to extrapolate our  $I_{LT}^n(Q^2)$  to  $Q^2 = 0$  and provided that the GDH relation is correct, which is widely expected and supported by dedicated experimental studies [27], our data satisfy Schwinger's prediction that  $I_{LT}^n(0) = 0$  [17]. Our trend contrasts with the MAID model and presumably the  $\chi$ EFT calculations, since MAID tracks those (see Fig. 3). This suggests that the problem lies in the theoretical description of the neutron structure.

Integrands: The integrands (excluding the  $\nu$ -weighting) of  $\delta_{LT}^n(Q^2)$ ,  $I_{LT}^n(Q^2)$  and  $\gamma_0^n$ , are displayed in Figs. 6 and 7.

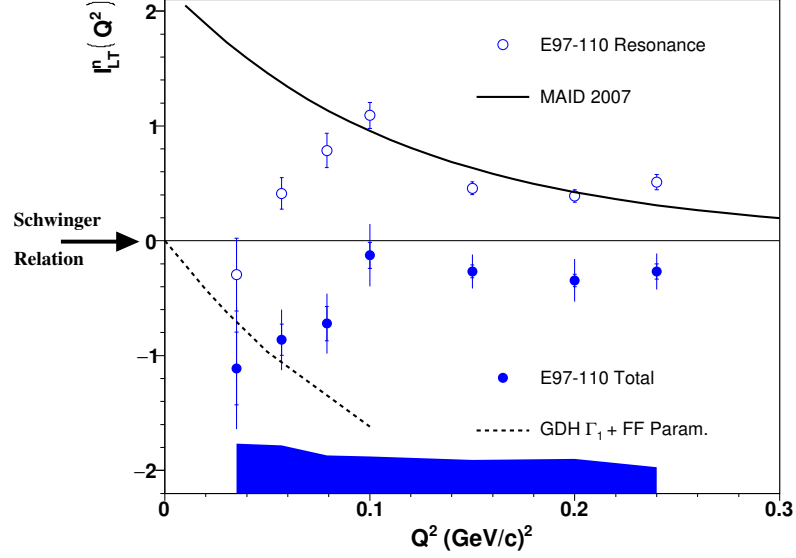


FIG. 5: The  $I_{LT}^n(Q^2)$  integral. The open symbols are our results without the large  $\nu$  part of  $I_{LT}$ . The filled blue circles are our results for the full  $I_{LT}$ , using an estimate for the large  $\nu$  contribution. The inner error bars represent the statistical uncertainties. The outer error bars show the combined statistical and uncorrelated systematic uncertainties. The correlated systematic uncertainty is indicated by the band. The Schwinger relation [17] for the neutron predicts  $I_{LT}^n(0) = 0$  at  $Q^2 = 0$ . The plain line shows the MAID model [15] (resonance only, to be compared to the open symbols). The dashed line uses the GDH [28, 29] and Burkhardt-Cottingham [20] relations, together with an elastic form factor parameterization [26], to obtain  $I_{LT}^n(Q^2)$  for  $Q^2 \rightarrow 0$ .

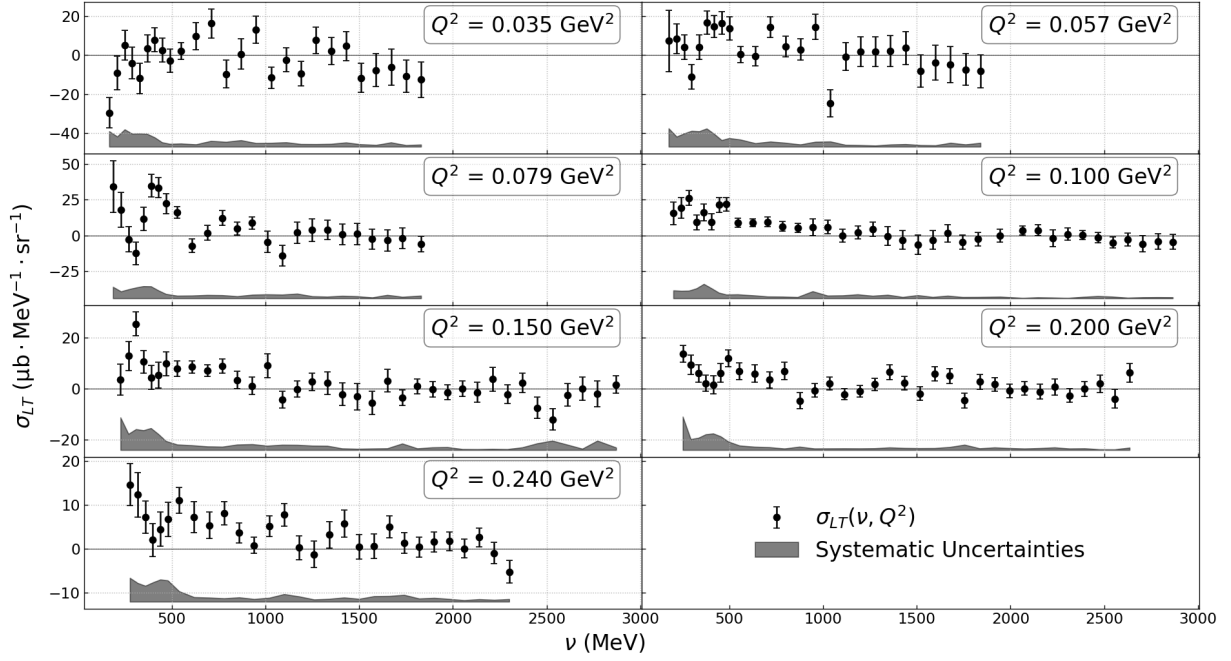


FIG. 6: The longitudinal-transverse interference cross-section  $\sigma_{LT}(\nu, Q^2)$  for  $^3\text{He}$  at the  $Q^2$  values at which it is integrated into  $\delta_{LT}(Q^2)$  (Eq. 2) or  $I_{LT}(Q^2)$  (Eq. 3). The nuclear corrections [23] necessary to obtain the neutron information from the  $^3\text{He}$  data are applied after the integration. The prominent  $\Delta(1232)$  contribution seen for  $\sigma_{TT}(\nu, Q^2)$  in Fig. 7 is not present here, in agreement with the expectation that the role of  $\Delta(1232)$  is suppressed in LT-interference quantities.

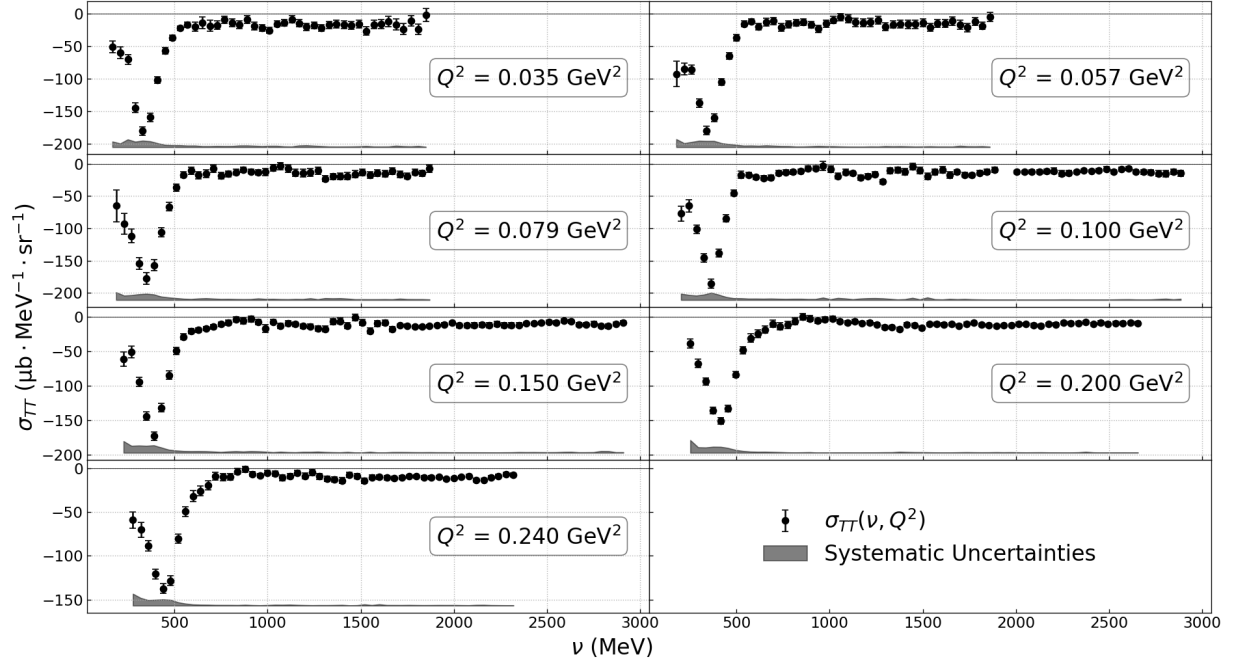


FIG. 7: The transverse-transverse cross-section  $\sigma_{TT}(\nu, Q^2)$  for  $^3\text{He}$  at the  $Q^2$  values at which it is integrated to form  $\gamma_0$  (Eq. 1). The nuclear corrections providing the neutron information from the  $^3\text{He}$  data are applied after the integration. The prominent negative peak at small- $\nu$  is the  $\Delta(1232)$  contribution.



Data table

$Q^2$	$x_{min} (W_{max})$	$\gamma_0^n(Q^2) \pm (\text{stat}) \pm (\text{syst})$	$\delta_{LT}^n(Q^2) \pm (\text{stat}) \pm (\text{syst})$	$I_{LT}(Q^2)^n \pm (\text{stat}) \pm (\text{syst})$	$\frac{I_{LT}^{meas.}}{I_{LT}}$
0.035	0.0112 (2.00)	$-3.094 \pm 0.129 \pm 0.270$	$-0.383 \pm 0.326 \pm 0.677$	$-1.112 \pm 0.316 \pm 0.606$	0.26
0.057	0.0181 (2.00)	$-3.117 \pm 0.141 \pm 0.259$	$0.225 \pm 0.071 \pm 0.197$	$-0.862 \pm 0.136 \pm 0.389$	-0.48
0.079	0.0249 (2.00)	$-2.717 \pm 0.140 \pm 0.270$	$0.435 \pm 0.098 \pm 0.195$	$-0.721 \pm 0.149 \pm 0.314$	-1.09
0.100	0.0183 (2.50)	$-2.070 \pm 0.074 \pm 0.170$	$0.491 \pm 0.083 \pm 0.209$	$-0.126 \pm 0.114 \pm 0.329$	-8.65
0.150	0.0273 (2.50)	$-1.370 \pm 0.051 \pm 0.125$	$0.215 \pm 0.052 \pm 0.173$	$-0.266 \pm 0.057 \pm 0.233$	-1.72
0.200	0.0398 (2.40)	$-0.965 \pm 0.032 \pm 0.065$	$0.111 \pm 0.028 \pm 0.091$	$-0.345 \pm 0.055 \pm 0.267$	-1.13
0.240	0.0547 (2.25)	$-0.742 \pm 0.026 \pm 0.050$	$0.108 \pm 0.020 \pm 0.043$	$-0.267 \pm 0.067 \pm 0.192$	-1.91

TABLE I: Data and kinematics. From left to right: Four-momentum transfer ( $[\text{GeV}]^2$ ); minimum  $x \equiv Q^2/2m\nu$  value experimentally covered (equivalent maximum invariant  $W[\text{GeV}]$  ( $W = (M^2 + 2M\nu - Q^2)^{1/2}$ );  $\gamma_0^n(Q^2) \pm \text{statistical uncertainty} \pm \text{systematic uncertainty}$ ;  $\delta_{LT}^n(Q^2) \pm \text{statistical uncertainty} \pm \text{systematic uncertainty}$ ;  $I_{LT}(Q^2)^n$ , including an estimate for the unmeasured contribution below  $x_{min}$ ,  $\pm \text{statistical uncertainty} \pm \text{systematic uncertainty}$ ; Ratio of measured to total  $I_{LT}(Q^2)^n$ . The unmeasured parts of  $\gamma_0^n(Q^2)$  and  $\delta_{LT}^n(Q^2)$ , i.e, the contributions for  $x < x_{min}$ , are entirely negligible.